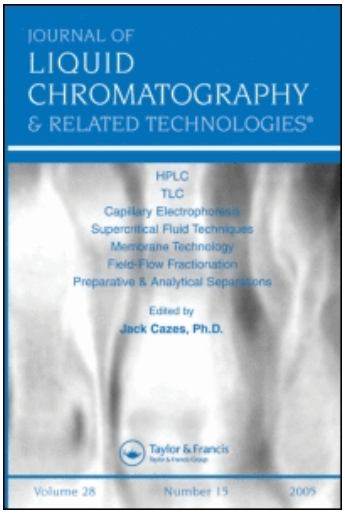

Journal of Liquid Chromatography & Related Technologies
Publication details, including instructions for authors and subscription information:
http://www.informaworld.com/smpp/title~content=t713597273

HYDRODYNAMIC CHROMATOGRAPHY IN NARROW AND WIDE-BORES; WHETHER RADIAL DIFFUSION IS ESSENTIAL OR NOT

Tetsuo Okada[a]
[a] Department of Chemistry, Tokyo Institute of Technology, Tokyo, Japan

Online publication date: 14 July 2010

To cite this Article Okada, Tetsuo(2010) 'HYDRODYNAMIC CHROMATOGRAPHY IN NARROW AND WIDE-BORES; WHETHER RADIAL DIFFUSION IS ESSENTIAL OR NOT', Journal of Liquid Chromatography & Related Technologies, 33: 9, 1116 — 1129
To link to this Article: DOI: 10.1080/10826076.2010.484351
URL: http://dx.doi.org/10.1080/10826076.2010.484351

Journal of Liquid Chromatography & Related Technologies, 33:1116–1129, 2010

ISSN: 1082-6076 print/1520-572X online
DOI: 10.1080/10826076.2010.484351

Taylor & Francis
Taylor & Francis Group

HYDRODYNAMIC CHROMATOGRAPHY IN NARROW AND WIDE-BORES; WHETHER RADIAL DIFFUSION IS ESSENTIAL OR NOT

Tetsuo Okada

Department of Chemistry, Tokyo Institute of Technology, Tokyo, Japan

□ *Methodological features of hydrodynamic chromatography (HDC) both in narrow and wide-bores are discussed in this review. HDC in narrow-bore allows separation of particles or macromolecules having relatively large dimensions; whereas, wide-bore HDC (W-HDC) allows separation of even small molecules only if they have one-order different intrinsic diffusivity. Main focus is on the latter method. This method relies on the diffusion of analytes and laminar flow. Since a stable and well-defined laminar flow is established in a capillary, it is a suitable platform of W-HDC. We discuss the basic principles followed by some applications. In addition, the strategy for rapid separation is discussed on the basis of a convenient parameter derived from the advection-diffusion equation. Separation in the sub second range is possible with W-HDC by appropriate reduction of the system dimension.*

Keywords diffusion of analytes, particle separation, rapid separation, wide-bore hydrodynamic chromatography

A number of instrumental separation techniques have been developed based on various principles and concepts. Chromatography, electrophoresis, and field flow fractionation (FFF) are representative separation methods, which have found many applications in current chemistry and its related disciplines. There are two common features involved in these methodologies; for example, they rely on the interaction of analytes in a separation field and on a fluid flow therein. The differentiation of the mobility between analytes by a field interaction results in discrete peaks, which are usually monitored by a detector placed downstream. Chemical interactions between analytes and stationary phases are employed in chromatography to create a difference in the mobility between analytes. On the other hand, physical forces are utilized in electrophoresis and

Address correspondence to Tetsuo Okada, Department of Chemistry, Tokyo Institute of Technology, Meguro-ku, Tokyo 152-8551, Japan. E-mail: tokada@chem.titech.ac.jp

FFF. An electric force is the primary field interaction in electrophoresis, and various physical forces, such as electric, thermal, cross flow, and sedimentation, act as an external field in FFF[1,2] and its related techniques.[3,4] Although there is a difference in the intrinsic properties of a field, these methods (i.e., chromatography, electrophoresis, and FFF), have common methodological features; in fact, many chromatographers are working on electrophoresis as well.

Another important feature common to these separation techniques is that they strongly rely on a fluid flow, though the role of a fluid flow is quite different. In typical chromatography, a fluid flow carries a solute along a column to a detector. Since the flow should pass through the interstitials between stationary phase materials, no attention is usually paid to the flow profile across the column. Although an electroosmotic flow occurring in an electric field is not essential for electrophoretic separation, the enhanced mobility of analytes sometimes allows us to detect them, which otherwise never reach the detector possibly due to very small mobility or that they are in the opposite direction. A narrow solute zone can be kept in an electroosmotic flow because of it plug flow profile, unlike a pressurized flow. This nature is one of the reasons that high separation performance is accomplished in capillary electrophoresis or capillary electrochromatography. In contrast, FFF separation strongly relies on the profile of a laminar flow, which occurs under the condition of a low Reynolds number. Since working in a small space results in the reduction of the Reynolds number of a system, a microchip can be a good platform for FFF.[5]

Hydrodynamic chromatography (HDC) is not a prevalent method in comparison with the methods stated previously but is known as an effective technique for separation of particles and macromolecules.[6–14] As discussed later, an attractive feature of this method is that no apparent field interaction is involved in its separation mechanism. The sizes of analytes should be larger than a few percent of that of a capillary (or the thickness of a separation channel) for separation to occur. Therefore, we have to adjust the size of a separation system for the dimension of analytes that we wish to separate on the basis of this mechanism. In this separation, the radial diffusion of an analyte is ignored because it is thought to be insignificant. In contrast, the radial diffusion of an analyte plays an essential role in wide-bore capillary hydrodynamic chromatography (W-HDC).[15–18] Separation occurs under the conditions that the usual HDC mechanism does not work. HDC and W-HDC are thus complementary from the perspective of the ratio of the analyte size to the system dimension. These methods follow theoretical consideration because no external fields are involved in the separation mechanism. This feature allows simple designs of a separation systems and easy prediction of the behavior of analytes. In this review, the principles and state-of-the-art uses of these separation modes are briefly

reviewed, and the main focus is on W-HDC as thourough review papers on HDC have already been published.[14]

HDC

HDC is a classical method, which has been used for separation of polymers and particles. Although Boss and Tijssen[14] already reviewed HDC for polymer separation in detail, HDC deserves short statements to see a difference between HDC and W-HDC. Using a laminar flow in an open capillary as the simplest case, which follows the hydrodynamic theory thoroughly, produces results as shown in Figure 1. The flow profile is described by the Hagen-Poiseuille equation.

$$u(r) = \frac{2\bar{u}}{a^2}(a^2 - r^2) = u_{\max}\left(1 - \frac{r^2}{a^2}\right) \tag{1}$$

where $u(r)$ is the linear flow rate at the radial coordinate, r, a is the radius of the capillary, and $\bar{u}$ and $u_{\max}$ are the average and maximum linear flow rate, respectively. The average flow velocity can also be represented by:

$$\bar{u} = \frac{2\pi \int_0^a u(r) r dr}{\pi a^2} \tag{2}$$

Although small molecules utilize the entire volume of the interior of a capillary, the gravity center of an analyte with a relatively large size cannot approach to the capillary wall. For an analyte with the radius, R, the flow velocity can be written as:

$$u_p = \frac{2\pi \int_0^{a-R} u(r) r dr}{\pi (a - R)^2} = \bar{u}(1 + 2\lambda - \lambda^2) \tag{3}$$

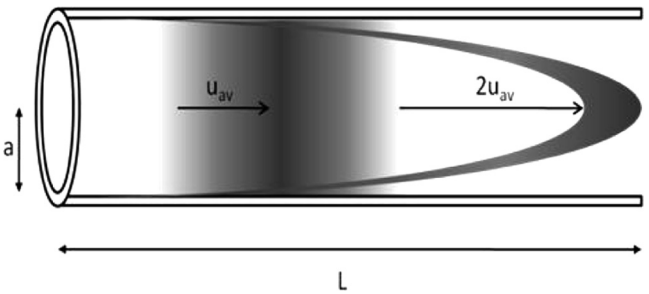

FIGURE 1 Schematic representation of a laminar flow profile and the movements of a diffusive and nondiffusive analytes through a tube.

where $\lambda = R/a$. An appropriate coefficient for λ^2 has been attempted to make a correction for effects such as the rotation of a particle.

This separation was carried out in an open capillary or a packed column. The former suits fundamental studies to confirm the agreements between theories and experiments but is not useful for practical separation. In addition, to separate nanoparticles or polymers, we need a submicrometer gap, which was difficult to realize with classical chromatography and its related techniques. Therefore, early studies of HDC were mostly conducted with packed columns. A simple model described previously does not hold for such cases, because a well-defined laminar flow is not established therein, though the basic concept must still be correct.

In contrast, the recent developments of this separation mode are remarkable, which have been enabled by the advancements of micro machining technologies.[9,10] A flat cell with the depth of 1 μm was fabricated on a silicon chip and was attempted for nanoparticle separation. Surprisingly, high separation efficiency was realized by constructing a microstructure of suitable geometry, which allows the injection of a sample of 150 pL. This advancement has opened a new era for HDC as a high performance separation tool.

Advection Involving Diffusion Effects

HDC assumes the fast diffusion of analytes over the cross section of a separation channel. In actuality, analytes may undergo diffusion in directions parallel and perpendicular to the flow direction. This effect is particularly important for large analytes with low intrinsic diffusivity. Particles, which are often targeted analytes in HDC, mostly have small diffusion coefficients (D). The Einstein-Stocks equation allows the estimation of D for a particle with the radius, R, in a medium of the viscosity, η

$$D = kT/6\pi\eta R \tag{4}$$

where k and T are the Blotzmann constant and temperature. According to this equation, the diffusion coefficients for 10 nm and 100 nm particles in water can be estimated to be 4.38×10^{-11} and $4.38 \times 10^{-12}\,m^2\,s^{-1}$, respectively.

One dimensional mean-square displacement (σ^2) by diffusion is given by the following equation.

$$\sigma^2 = 2Dt \tag{5}$$

When 10 nm particles travel through a capillary of $r = 100\,\mu m$, it takes ca 100 s for particles flowing at the center of the capillary to diffuse across the entire capillary cross-section to the wall. The time required for the

diffusion of dissolved small solutes, which usually have at least one order larger diffusion coefficient than a 10 nm particle, is reduced to 10 s; this time regime is long enough to eliminate problems coming from the nonequilibrium of analyte diffusion in a usual separation system.

However, if we work with a high flow rate and with a large bore capillary, the complete diffusion over the entire cross section is not necessarily accomplished even for dissolved solutes within a short time period. This has been a motivation for analytical chemists to understand the mass transfer in a capillary on the basis of the advection-diffusion equation. The numerical calculation of the advection-diffusion equation was reported by Vanderslice[19] and Korenaga[20–22] to understand the molecular behavior in the systems of flow injection analysis. They utilized the equation devised by Taylor[23]

$$D\left(\frac{\partial^2 C}{\partial x^2}+\frac{\partial^2 C}{\partial r^2}+\frac{1}{r}\frac{\partial C}{\partial r}\right)=\frac{\partial C}{\partial t}+u(r)\frac{\partial C}{\partial x} \tag{6}$$

This equation was derived from the mass balance in a small segment as a part of a cylinder. Harada et al.[16,18] have also numerically analyzed this equation with reduced parameters, $z=r/a$, $\tau=Dt/a^2$, and $\chi=Dx/(a^2u_{max})$. The entire capillary was divided into 9600 cells (40×240, radial and axial meshes), and the solute concentrations in each cell was calculated. The integrated concentration at the 236th axial cells from the inlet was assumed as a detector response. The centered difference method was used for the analysis of the diffusion term, $D\left(\frac{\partial^2 C}{\partial x^2}+\frac{\partial^2 C}{\partial r^2}\right)$, whereas the cubic interpolated pseudoparticle (CIP) method was applied to solve the advection term, $\frac{\partial C}{\partial t}+u(r)\frac{\partial C}{\partial x}-\frac{D}{r}\frac{\partial C}{\partial r}$. CIP is known as one of the suitable methods for numerical analyses of differential equations and is capable of providing stable results without severe losses of conservation. This property of CIP allows us to reduce the number of theoretical cells and, in turn, times necessary for simulation.

Figure 2 shows simulated elution curves obtained under different conditions. To facilitate the discussions, a parameter, $\tau_{av}=DL/(a^2u_{av})$, was defined, which represents the solute diffusivity in the system, where L is the length of a capillary. If $\tau_{av}=1$, $\sigma^2=2a^2$, indicating that the solute can diffuse over the entire cross-section of capillary within the time of $t/2$. This means that the solute traveling at the maximum flow rate, which is twice as large as the average flow rate, can completely diffuse before it is eluted from the capillary. The elution curves calculated for $\tau_{av}=0.041$–2.26 are compared in Figure 2. As is well known, if solute diffusion is completed, the peak profile can be described by a Gaussian distribution curve. We can see such symmetric curves for $\tau_{av}>1$. As τ_{av} decreases, the peak becomes broad, and then a new peak, named a non-diffusion peak, appears. This peak has half the elution time of the diffusion peak and thus

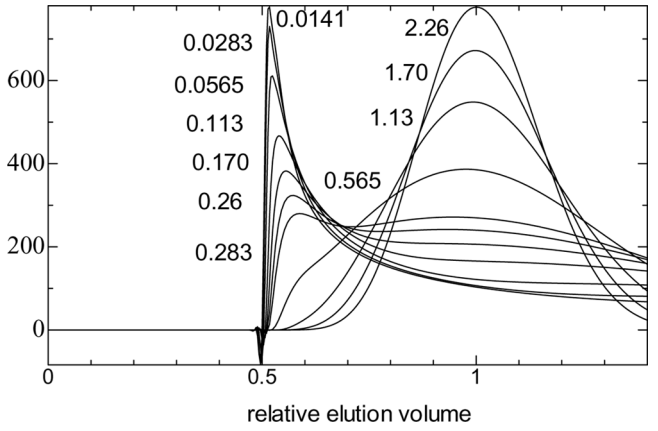

FIGURE 2 Simulated elution curves for analytes with different diffusivities. The values of τ_{av} are labeled on the elution curves.

reflects the movement of solutes at the maximum flow rate. The non-diffusion peak becomes sharp for $\tau_{av} < 0.1$, and then the diffusion peak becomes negligible.

The calculations were compared with experiments. Figure 3 shows the elution curves of a sodium dedecylsulfate micelle doped with pyrene to enable UV detection. Changing either the flow rate (u_{av}) or a capillary radius (a) allows us to vary τ_{av} values. The flow rate was varied from $0.83\,\mathrm{mm\,s^{-1}}$ ($\tau_{av} = 1.06$) to $4.1\,\mathrm{mm\,s^{-1}}$ ($\tau_{av} = 0.21$) in Figure 3a. A Gaussian-shaped peak appears with the lowest flow rate; whereas, a nondiffusion peak can be seen at the elution volume of 20 μL with $u_{av} = 4.1\,\mathrm{mm\,s^{-1}}$. Similarly, enlarging the capillary radius resulted in the appearance of a skewed nondiffusion peak even with the constant linear flow rate as shown in Figure 3b. These indicate the good agreements between the simulation (Figure 2) and the experiments (Figure 3). Thus, it was confirmed that τ_{av} is a good measure to represent the system diffusion of an analyte, which is determined by the dimensions of a capillary and a flow rate as well as the diffusion coefficient of an analyte.

W-HDC Separation

The simulations and experiments shown in the preceding section imply that the simple passage of analytes possibly provides two peaks under the condition that one analyte behaves as a diffusive one and another as a non-diffusive one. Although a nondiffusive analyte is eluted ahead of a diffusive one, the complete elution of the former takes a very long time. Therefore, the emergence of two peaks does not mean real separation of these

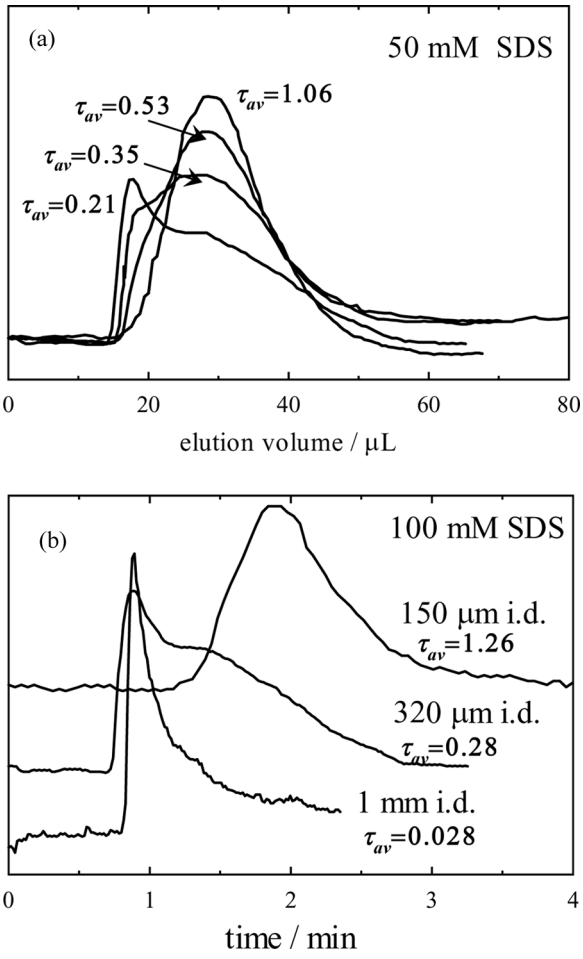

FIGURE 3 Elution curves of SDS micelles under various conditions; (a) effect of flow rate and (b) effect of capillary radius. (a) 50 mM SDS eluted from 320 μm i.d. capillary with average linear flow rates (u_{av}) ranging from 0.83 mm s^{-1} ($\tau_{av}=1.06$) to 4.1 mm s^{-1}($\tau_{av}=0.21$). (b) 100 mM SDS eluted with $u_{av}=2.7$ mm s^{-1} from capillaries with various radii.

analytes. However, it would be of analytical value to resolve two analytes as two discrete peaks by simple passage through an open capillary.

The simulation shown in Figure 2 indicates that an analyte with $\tau_{av}=0.1$ gives a nondiffusion peak while that with $\tau_{av}=1$ appears as an almost symmetric diffusion peak. This means that two analytes can be resolved by controlling conditions only if they have one order different diffusion coefficients. Figure 4 shows the resolution between I^- and a 0.6 μm PS particle. Since the former have larger diffusion coefficients than the latter by ca. two orders of magnitude, two discrete peaks appear.

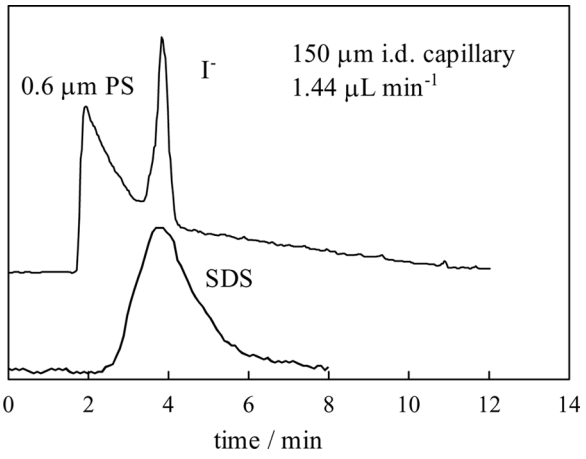

FIGURE 4 Elution curves of test analytes 150 μm i.d. × 0.3 m capillary was used. Mobile phase flow rate, 1.44 μL min^{-1}, corresponding to $u_{av} = 1.36\,mm\,s^{-1}$. Sample volume, 0.15 μL. On-capillary detection at 220 nm.

Thus, an advantage of this method is that the system diffusion of a given analyte can be altered by changing the dimensions of a capillary and a flow rate of a running solution. However, such separation is not obviously possible unless the diffusion properties of analytes differ by at least one order of magnitude. Since dissolved small molecules typically have the diffusion coefficients of $\sim 10^{10}\,m^2\,s^{-1}$, their separation appears impossible with this principle. This methodological limitation has been overcome by the utilization of the interaction of solutes with molecular aggregates.

Molecular aggregates, in general, have much smaller diffusion coefficients than small dissolved molecules, and, therefore, can behave as nondiffusive analytes under the conditions that allow the high diffusivity of small molecules. In micellar chromatography or micellar electrokinetic chromatography, micellar partition has been utilized for separation of various organic and inorganic solutes, involving those not separated without micelles. Similar utilization of molecular aggregates in W-HDC has allowed separation of dissolved molecules on the basis of this mechanism.[17] It has been shown that the incorporation of vesicles of dihexadecyldimethylammonium bromide in a running solution allows W-HDC separation of anthracene from naphthalene and I^- from NO_3^- as shown in Figure 5. As stated previously, separation in W-HDC is not completed under any conditions, and, thus, overlapping of two peaks is seen in both cases. However, it is noteworthy that this technique is applicable to the separation of such small molecules.

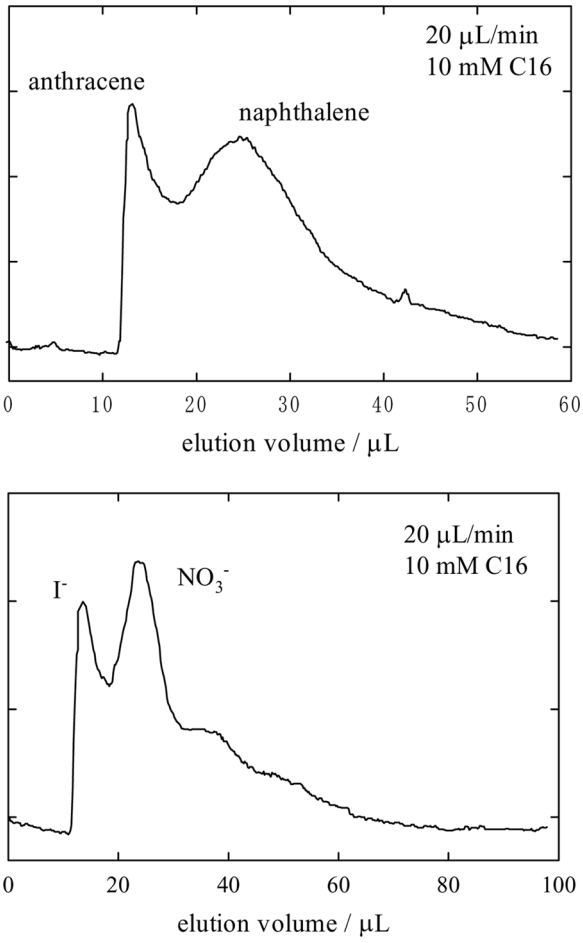

FIGURE 5 Resolution between anthracene and naphthalene (upper) and I^- and NO_3^- (lower) with 10 mM dihexadecyldimethylammonium bromide (C16) vesicular carrier. Average linear flow rate, 4.14×10^{-3} m sec^{-1}. Capillary, 320 mm i.d $\times$ 0.3 m.

Rapid W-HDC

Another important feature of W-HDC is its high potential in rapid separation. Since neither physical nor chemical interaction is involved in the separation mechanism of W-HDC, very high flow rates are applicable without causing unnecessary peak broadening coming from the kinetics of a retention equilibrium, and separation can be achieved within a very short distance. The strategy for rapid W-HDC based on τ_{av} is summarized in Figure 6, which shows relations between a and the elution time required for analytes of $D = 5 \times 10^{-10}$, 5×10^{-11}, and 5×10^{-12} m^2 s^{-1} to give diffusion peaks ($\tau_{av} = 1$). The L/u_{av} is taken as the abscissa instead of time

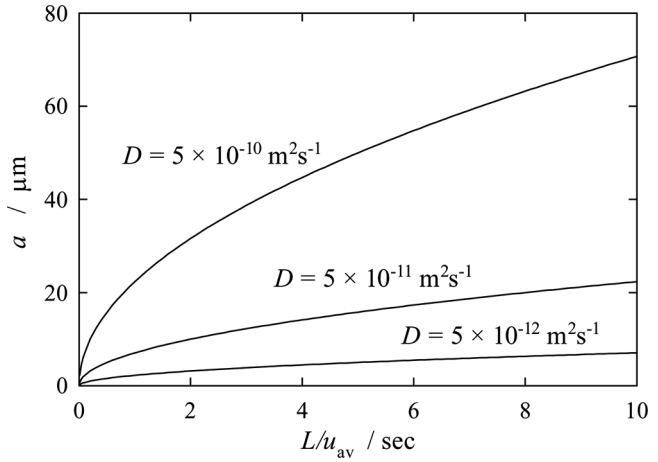

FIGURE 6 Relation between a and time required for analytes of various diffusivities to attain $\tau_{av} = 1.0$.

(L/u_{av} has the dimension of time). This means that changing the length of a capillary is complementary to changing a flow rate. With a relatively large capillary (e.g., $a = 50\,\mu m$), an analyte of $D = 5 \times 10^{-10}\,m^2\,s^{-1}$ gives a diffusion peak if the elution takes longer than 5 s. In contrast, those of $D = 5 \times 10^{-11}$ or $5 \times 10^{-11}\,m^2\,s^{-1}$ never behaves as a diffusive analyte in a 50 μm-capillary in the time range depicted in this figure (even with a 20 μm-capillary, they are almost non-diffusive).

Although the time required for an analyte to flow through a capillary is experimentally controlled in either changing a flow rate or the length of a capillary as stated previously, the former is a more convenient way. However, too high flow rates can cause a turbulent flow and too high pressure gradient. A use of a small-bore capillary reduces the Reynolds number and, in turn, reduces the possibility of a turbulent flow. However, a pressure gradient should be enhanced. A use of a short capillary eliminates these risks.

The time required for an analyte to be diffusive is proportional to a^{-2}, suggesting that the bore-size of a capillary is the most critical parameter and should first be optimized when fast W-HDC separation is designed. Figure 7 shows a modification of Figure 6, in which fluorescein (FL), 15 nm, and 320 nm PS particles are assumed as analytes. The curves 1 and 2 indicate the conditions giving $\tau_{av} = 1$ for FL and the 15 nm PS particle, respectively. If we select an appropriate condition that allows $\tau_{av} \leq 0.1$ for one and $\tau_{av} \geq 1$ for the other, the injection of a mixture should result in discrete peaks. The curve 3 in Figure 7 represents $\tau_{av} = 0.1$ for the 320 nm PS particle. Thus, two discrete peaks can be obtained under any condition between the curves 1 and 3 for FL and the 320 nm particle, and similarly between the curves 2 and 3 for the 15 nm and 320 nm particles. Horizontal

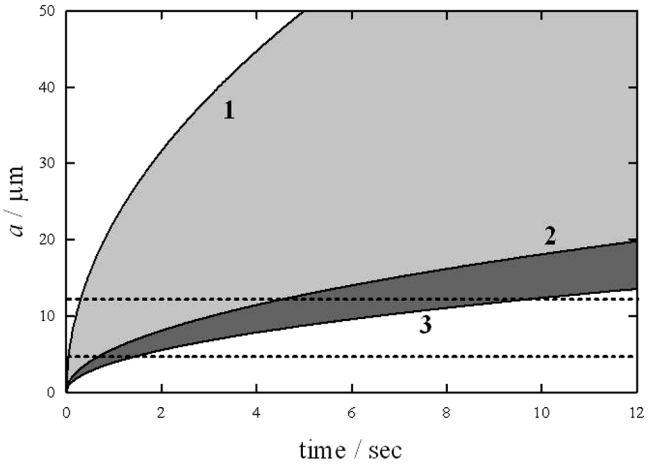

FIGURE 7 Optimization of rapid W-HDC conditions. Curves, (1) $\tau_{av}=1.0$ for FL, (2) $\tau_{av}=1.0$ for the 15 nm PS particle, and (3) $\tau_{av}=0.1$ for the 320 nm PS particle. Horizontal broken lines represent $a=5$ μm and 12.5 μm.

lines in this figure show the radii of commercially available 25 μm- and 10 μm-capillaries. Figure 6 tells us that the 10 μm-capillary is appropriate for the separation of the 15 nm and 320 nm particles, whereas, both the 10 μm- and 25 μm-capillaries can be used for the separation of FL and the 320 nm PS particle.

Figure 8 compares the separation of the 15 nm and 320 nm particles with these two capillaries of different bore sizes.[24] As discussed previously, the particles are separated for ca. 0.5 sec with the 10 μm-capillary, while the same separation required ca. 7 sec with the 25 μm-capillary. Figure 9 shows

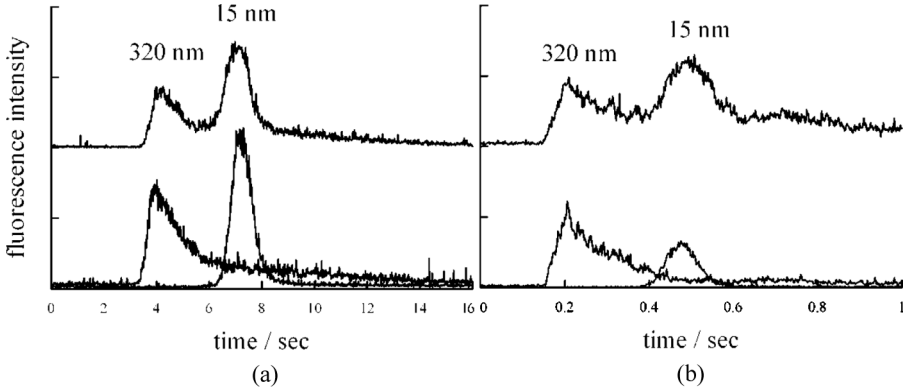

FIGURE 8 Wide-bore HDC separation of the 15 nm and 320 nm PS particles. Capillary, (a) $a=12.5$ μm and $L=2.5$ mm, (b) $a=5$ μm and $L=2.5$ mm. The upper curves were obtained with the injection of a mixture, while the lower curves correspond to individual injections.

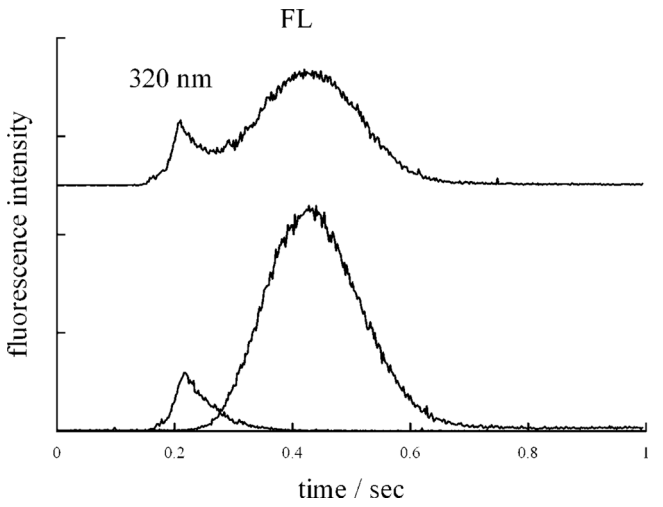

FIGURE 9 Wide-bore HDC separation of FL and the 320 nm PS particles. Capillary, $a = 12.5\,\mu m$ and $L = 2.5\,mm$. The upper curves were obtained with the injection of a mixture, while the lower curves correspond to individual injections.

the sub-second separation of FL and the 320 nm PS particle with the 25 μm-capillary.

Another technological key issue of the rapid W-HDC is the injection of a sample into a capillary. Micromachining technology has allowed the fabrication of various types of injection devises on a chip for HDC or electrophoresis.[9,10,25,26] It is one of the advantages to the use of a capillary such that simple injection methods are applicable. For the measurements of elution curves depicted in Figures 8 and 9, a PTFE plate was used for sample injection. Sample and running solution drops were kept on the plate, and one end of a capillary touched the drop of the running solution. The solution flow was driven by a pump operated in a suction mode. Thus, the running solution was drawn into the capillary at a constant rate. The PTFE plate was quickly moved between two droplets, and the sample solution was injected as a plug by a short contact between the capillary tip and the sample drop. The manual operation allowed the injection of a small volume of a sample for subsecond separation. However, the time lag of tens of microseconds was unavoidable. An automatic system rather than manual one is necessary for faster separation.

CONCLUSION

Hence, HDC in narrow- and wide-bores has been reviewed. For narrow-bore HDC separation, the gap of a separation channel should be smaller than 100 times the size of the analytes. The mechanism of HDC

does not work with a larger gap because the exclusion volume near the channel wall becomes negligible in comparison with the entire volume of a separation channel. When a typical HDC mechanism does not contribute to the differentiation of analytes due to the excessively large size of the channel gap, the diffusion mechanism becomes dominant in W-HCD. W-HDC is thus complementary to the usual HDC from the viewpoint of the relative dimensions of analytes to the separation channel.

Although the application of W-HDC is now very restricted because of its low separation performance, its instrumental simplicity and compatibility to rapid separation will lead to a high potential to open new applications of this uncommon method. As shown in this review, sub second separation has been reported. According to the strategy for the reduction of a separation time, faster W-HDC separation would be possible. However, an appropriate injection scheme should be developed to move to shorter time regimes. Millisecond separation must be feasible by W-HDC with an appropriate injection device, which allows us to visualize the reactions with the first-order reaction rates of $k \sim 100\,\mathrm{s}^{-1}$ by separation.

REFERENCES

1. Roda, B.; Zattoni, A.; Reschiglian, P.; Moon, M.H.; Mirasoli, M.; Michelini, E.; Roda, A. Field-flow fractionation in bioanalysis: A review of recent trends. Anal. Chim. Acta. **2009**, *635*, 132–143.
2. Williams, S.K.R.; Lee, D. Field-flow fractionation of proteins, polysaccharides, synthetic polymers, and supramolecular assemblies. J. Sep. Sci. **2006**, *29*, 1720–1732.
3. Suwa, M.; Watarai, H. Magnetophoretic evaluation of interfacial adsorption of dysprosium(III) on a single microdroplet. Anal. Sci. **2008**, *24*, 133–137.
4. Masudo, T.; Okada, T. Microparticle separation with acoustic-gravity field controlled by phase-shift operation. Anal. Sci. **2007**, *23*, 385–387.
5. Edwards, T.; Gale, B.K.; Frazier, A.B. A microfabricated thermal field flow fractionation system. Anal. Chem. **2002**, *74*, 1211–1216.
6. Ploehn, H.J. Lateral migration mechanism in capillary hydrodynamic chromatography. Int. J. Multiphase Flow **1987**, *13*, 773–784.
7. Mullins, M.E.; Orr, C. Particle sizing by capillary hydrodynamic chromatography. Int. J. Multiphase Flow **1979**, *5*, 79–85.
8. Takauchi, T.; Siswoyo; Aspanut, Z.; Lim, L.W. Hydrodynamic chromatography of silica colloids on small spherical nonporous silica particles. Anal. Sci. **2009**, *25*, 301–306.
9. Chmela, E.; Tijssen, R.; Blom, M.T.; Gardeniers, H.J.G.E.; van den Berg, A. A chip system for size separation of macromolecules and particles by hydrodynamic chromatography. Anal. Chem. **2002**, *74*, 3470–3475.
10. Blom, M.T.; Chmela, E.; Oosterbroek, R.E.; Tijssen, R.; van den Berg, A. On-chip hydrodynamic chromatography separation and detection of nanoparticles and biomolecules. Anal. Chem. **2003**, *75*, 6761–6768.
11. Stegeman, G.; van Asten, A.C.; Kraak, J.C.; Poppe, H.; Tijssen, R. Comparison of resolving power and separation time in thermal field-flow fractionation, hydrodynamic chromatography, and sze-exclusion chromatography. Anal. Chem. **1994**, *66*, 1147–1160.
12. Stegeman, G.; Kraak, J.C.; Poppe, H.; Tijssen, R. Hydrodynamic chromatography of polymers in packed columns. J. Chromatogr. A **1993**, *657*, 283–303.
13. Blom, M.T.; Chmela, E.; Gardeniers, J.G. E.; Tijssen, R.; Elwenspoek, M.; van den Berg, A. Design and fabrication of a hydrodynamic chromatography chip. Sensor. Actuator. B **2002**, *B82*, 111–116.

14. Boss, J.; Tijssen, R. Hydrodynamic Chromatography of Polymers, in *Chromatography in the Petroleum Industry*; Adlard, E.R., Ed.; Elsevier: London, 1995; 95–126.
15. Fischer, Ch.-H.; Giersig, M. Analysis of colloids VII. Wide-bore hydrodynamic chromatography, a simple method for the determination of particle size in the nanometer size regime. J. Chromatogr. A **1994**, *68*, 97–105.
16. Harada, M.; Kido, T.; Masudo, T.; Okada, T. Solute distribution coupled with laminar flow in wide-bore capillaries: What can be separated without chemical or physical fields? Anal. Sci. **2005**, *21*, 491–496.
17. Okada, T.; Harada, M.; Kido, T. Resolution of small molecules by passage through an open capillary. Anal. Chem. **2005**, *77*, 6041–6046.
18. Harada, M.; Kido, T.; Okada, T. Simulation of separation process with laminar flow in an open capillary. Bunseki Kagaku **2005**, *54*, 1161–1168.
19. Vanderslice, J.T.; Rosenfeld, A.G.; Beecher, G.R. Laminar-flow bolus shapes in flow injection analysis. Anal. Chim. Acta. **1986**, *179*, 119–129.
20. Korenaga, T. Rapid method for molecular diffusivity measurement of various inorganic chemicals based on laminar dispersion in capillary flow. Trends Inorg. Chem. **1991**, *2*, 189–196.
21. Korenaga, T.; Shen, F.; Takahashi, T. An experimental study of the dispersion in laminar tube flow. AIChE J. **1989**, *35*, 1395–1398.
22. Takahashi, T.; Korenaga, T.I.; Shen, F. A numerical solution for the dispersion in laminar flow through a circular tube. Can. J. Chem. Eng. **1990**, *68*, 191–196.
23. Taylor, G. Dispersion of soluble matter in solvent flowing slowly through a tube. Proc. Roy. Soc. A. **1953**, *219*, 186–203.
24. Umehara, R.; Harada, M.; Okada, T. Wide-bore hydrodynamic chromatography in sub-second range. J. Sep. Sci. **2009**, *32*, 472–478.
25. Chmela, E.; Blom, M.T.; Gardeniers, J.G.E.; van den Berg, A.; Tijssen, R. A pressure driven injection system for an ultra-flat chromatographic microchannel. Lab Chip. **2002**, *2*, 235–241.
26. Zhang, T.; Fang, Q.; Du, W.-B.; Fu, J.L. Microfluidic Picoliter-scale translational spontaneous sample introduction for high-speed capillary electrophoresis. Anal. Chem. **2009**, *81*, 3693–3698.